Application of Ultra-Thin Assembled Planar Metamaterial for Wireless Power Transfer System

**Junfeng Chen[1], Zhaoyang Hu[1], Shengming Wang[1], Minghai Liu[1, *],
Yongzhi Cheng[2], Zhixia Ding[3], Bin Wei[4], and Songcen Wang[4]**

Abstract—Magnetically coupled resonant wireless power transfer (WPT) has been employed in many applications, including wireless charging of portable electronic devices, electric vehicles, etc. However, the power transfer efficiency (PTE) decreases sharply due to divergence of magnetic field. Electromagnetic (EM) metamaterial (MM) can control the direction of magnetic fields due to its negative effective permeability. In this paper, MMs with negative effective permeability at radio frequencies (RF) are applied to a WPT system operating at around 16.30 MHz for improvement of PTE. This ultra-thin and assembled planar MM structure consists of a single-sided periodic array of the capaci-tively loaded split ring resonators (CLSRRs). Both simulation and experiment are performed to cha-racterize the WPT system with and without MMs. The results indicate that the contribution of high PTE is due to the property of negative effective permeability. By integrating MM in the WPT system, the experimental results verify that the measured PTE with one and two MM slabs have respectively 10% and 17% improvement compared to the case without MM. The measured PTEs of the system at different transmission distances are also investigated. Finally, the proposed MM slabs are applied in a more practical WPT system (with a light bulb load) to reveal its effects. The results verify the efficiency improvement by the realized power being transferred to the load.

1. INTRODUCTION

Wireless power transfer (WPT) technology was first proposed by Nikola Tesla more than 100 years ago [1]. In general, the approaches to wireless energy transfer can be categorized as near-field and far-field. To date, there have been mainly three methods for WPT, namely radiant WPT technology, inductive coupling WPT technology and resonant coupling WPT technology [2, 3]. Over the past several years, the near-field non-radiative WPT has sparked much interest due to its relatively large transfer distance and high power transfer efficiency (PTE), which has potential applications such as portable electronic devices, electric vehicles and powering of implanted biomedical devices. The mid-range non-radiant WPT technology was first proposed by Kurs et al. [4]. This technology is based on magnetic resonance theory and relies on near-field resonant coupling. The magnetic resonances are particularly suitable for daily applications because the interactions with environmental objects are reduced even further. So near-field magnetic resonance is more promising as a practical WPT technology. However, the PTE drops dramatically for distances larger than the diameter of the transfer coils [5].

In order to further extend the transfer distance and efficiency, the usage of metamaterial (MM) has been suggested. MM is an artificial composite medium that the electromagnetic (EM) properties can

be designed to achieve extraordinary phenomena not observed in the natural materials as, for instance, negative effective permittivity and permeability. Since 2000, Pendry and other researchers successively showed that a negative-index MM slab can refocus propagating waves and amplify evanescent waves, thus can be used to construct a "perfect lens," for imaging with theoretically unlimited resolution [6–8]. The properties of MMs, especially evanescent wave amplification, are of interest to WPT because the resonant coupling is essentially coupling of near-field evanescent waves. Very recently, theoretical analysis [9–14] and experiments [15–22] on MM to enhance the evanescent near-field and eventually improve the PTE in WPT systems have been reported. In 2010, a three-dimensional (3D) MM with a relative permeability equal to −1 was proposed by Choi and Seo [15]. It is reported that this MM structure was used as a magnetic flux guide in order to enhance the efficiency of energy transmission between a source and distant receiving coil. Urzhumov and Smith presented a theoretical analysis on the possibility of using MMs to enhance the mutual coupling between magnetic dipoles and thereby the efficiency of WPT system based on simplified assumptions [9, 11]. Wang et al. [16] showed that MM could be utilized to enhance the evanescent-wave coupling for enhancing power transfer. They were able to increase the transfer efficiency from 17% to 35% using 3D MM, at a moderate distance of 0.5 m. Previously reported MMs may be too thick and large in size to increase the power transfer distance and efficiency. In practical use, the big volume of 3D MMs may limit their applications. Zhao and Leelarasmee [12] focused on the design of thin MM slabs, but the experimental verification was not given. Therefore, a detailed investigation using planar and thin MM to enhance WPT is needed.

In this work, we numerically and experimentally investigate an ultrathin and assembled planar MM structure for 16.30 MHz WPT system, which consists of a single-sided periodic array of the capacitively loaded split ring resonators (CLSRRs) by an FR-4 substrate. The MM design is in very low frequency and is compact in size. In terms of wavelength at the operating frequency to unit cell ratio, the current design is about 153 while conventional split-ring resonator is around 10. The theoretical explanation and simulation of the divergent field focus and magnetic field enhancement are provided. At a distance of 30 cm, the measured PTEs with one and two MM slabs have respectively 10% and 17% improvement compared to a case without MM slab. The proposed structure is promising to be a good candidate using in WPT system with the advantages of light-weighted, ultrathin and fabrication simplicity.

2. METAMATERIAL DESIGN

To qualitatively interpret the principle of applying MM to WPT system and for the sake of simplicity, it is necessary to investigate how monochromatic plane-waves are effected, when transmitted through the MM slab. A system configuration for the calculation of transmission coefficients for MM slab is shown as Figure 1.
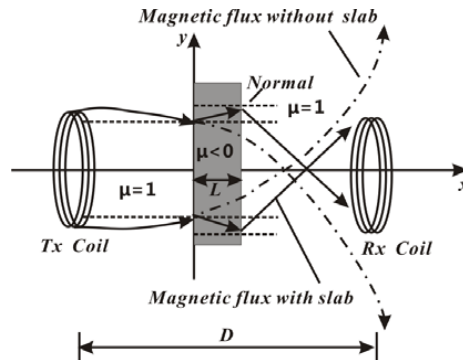

Figure 1. System configuration for the analysis of divergent field focus effect through MM slab.

In this analysis model, we assume that the MM slab is infinite in both y- and z-directions, and its planar boundaries are perpendicular to x-direction. The coils' magnetic flux contributes to WPT efficiency, i.e., only the magnetic field perpendicular to the plane of coil is effective. For simplicity, anisotropic MM only with manipulating H_x (perpendicular to MM slab) is sufficient to work for the

WPT system. Therefore, only the magnetic field along the x-axis needs to be considered. As we are mainly concerned with how the effective magnetic field component is affected by the MM, the original problem can be reduced to a one-dimensional (1D) case. To take transverse electric (TE) wave (with respect to the material interface) as an example, only three field components are nonzero: H_x, H_y, and E_z [12]. In different regions, the normal magnetic field components, H_x, can be expressed as:

$$H_x = \frac{E_0}{\omega\mu_y} e^{-jk_y y} \begin{cases} k_y(e^{-jk_x x} + Re^{jk_x x}), & x < 0, \\ q_y(Ae^{-jq_x x} + Be^{jq_x x}), & 0 \leq x \leq L, \\ k_y Te^{jk_x(x-L)}, & x > L, \end{cases} \tag{1}$$

The tangential electric and magnetic field components, E_z and H_y, can be expressed as:

$$H_y = \frac{E_0}{\omega\mu_y} e^{-jk_y y} \begin{cases} k_x(e^{-jk_x x} - Re^{jk_x x}), & x < 0, \\ q_x(Ae^{-jq_x x} - Be^{jq_x x}), & 0 \leq x \leq L, \\ k_x Te^{-jk_x(x-L)}, & x > L, \end{cases} \tag{2}$$

$$E_z = E_0 e^{-jk_y y} \begin{cases} e^{-jk_x x} + Re^{jk_x x}, & x < 0, \\ Ae^{-jq_x x} + Be^{jq_x x}, & 0 \leq x \leq L, \\ Te^{-jk_x(x-L)}, & x > L, \end{cases} \tag{3}$$

where E_0 is the magnitude of the incidence wave; k_x and k_y are wave numbers along x and y axis in free-space, respectively ($k_x^2 + k_y^2 = k_0^2$, where k_0 is the free-space wave number); q_x is the wave number along x-direction inside the MM slab; R and T are reflection and transmission coefficients; A and B are the amplitudes of waves inside the MM transmitting in forward and backward directions, respectively. By matching boundary conditions at $x = 0$ and $x = L$ so that the tangential field components (2) and (3) are continuous, the transmission coefficient can be calculated as

$$T = \frac{2q_x k_x}{(q_x + k_x)^2 e^{-jq_x L} - (q_x - k_x)^2 e^{jq_x L}} \tag{4}$$

Note that the above T is calculated from the front to back interface of the MM slab. Thus, the total T from the Tx coil to Rx coil planes taking into account wave propagation (decay for evanescent wave components) in the free-space region is given by

$$T' = \frac{2q_x k_x e^{-jk_x(D-L)}}{(q_x + k_x)^2 e^{-jq_x L} - (q_x - k_x)^2 e^{jq_x L}} \tag{5}$$

For μ-negative material ($\varepsilon = 1$, $\mu < 0$), q_x can be calculated as

$$q_x = \sqrt{\varepsilon\mu k_0^2 - k_y^2} \tag{6}$$

According to the theoretical analysis, application of the MM allows to reduce divergence of the bounded magnetic field and, therefore, to increase efficiency of the WPT system. As shown in Figure 1, divergent field decays exponentially on the direction of normal, which causes the field to exist only in a thin dielectric layer close to the vicinity of the surface. But the original attenuation field turns to enhancement field due to the inverse wave vector q_x. In formula (7), the wave vector q_x is purely imaginary in MM slab and therefore $-iq_x L > 0$. When negative μ approaches -1, it is obvious that the magnetic MM slab can focus the magnetic field and allows to reduce divergence of the bounded magnetic field.

$$\lim_{\mu \to -1} T = \lim_{\mu \to -1} \frac{2\mu q_x}{\mu q_x + q_x'} \frac{2q_x'}{q_x' + \mu q_x} \frac{\exp(iq_x' L)}{1 - \left(\frac{q_x' - \mu q_x}{q_x' + \mu q_x}\right)^2 \exp(2iq_x' L)} = \exp(-iq_x L) \tag{7}$$

In resonant coupling-based WPT systems, divergent magnetic field plays a key role. As mentioned above, application of the MM allows to reduce divergence of the bounded magnetic field and, therefore, to increase efficiency of the WPT system. It is reported that a negative-index MM slab can refocus divergence of the bounded magnetic field, thus can be used to construct a super-lens [23–25]. The field cannot amplify itself. The so-called field enhancement means that a MM acts as a near-field super-lens

to focus or concentrate the magnetoquasistatic field generated by the Tx coil source [6, 8, 10]. In fact, the total input energy is constant, but magnetic field is refocused or evanescent magnetic field component concentrated at the Rx coil so that the coupled magnetic flux density of Rx coil is enhanced compared with the case without MM [26]. Figure 1 shows a diagram of the field line distribution qualitatively with the anisotropic MM, where the modification of the field from a Tx is clearly visible, as well as the enhanced field strength near the receiver. The MM structure is used as a magnetic flux guide or repeater in order to enhance the magnetic field coupled by the Rx coil. In addition, the periodic field intensity of the magneto-static surface waves (MSW) on the surface of the MM can also be obtained (not shown) [10, 20, 27], illustrating the underlying coupled field shaping mechanism. Both these physical mechanisms for coupled magnetic field enhancement lead to a mutual coupling improvement between the Tx and Rx coils. The stronger the coupling is, the higher the WPT efficiency is. More intuitive analysis is also seen in the magnetic field simulation results in the following Section 3.

In general, a negative-index MM requires both effective permittivity ε and permeability μ to be negative. However, in deep sub-wavelength limit, the magnetic field and electric field decouple. According to above theoretical analysis, only μ is required to be negative to achieve divergent magnetic field amplification. Deep sub-wavelength MMs [25–30] generally operate at a relatively longer wavelength than their unit cell length. In this work, we have designed single-sided CLSRRs to achieve negative effective permeability. The designed MM has both the advantages of compact size and easy fabrication for WPT system. The CLSRRs are designed and optimized by CST Microwave Studio. Figure 2 shows the geometry of a unit cell for the CLSRRs. A lossy FR-4 substrate with relative permittivity $\varepsilon_r = 4.4$ and loss tangent $\tan\delta = 0.025$ is used. The metallic material is copper with electric conductivity $\sigma = 5.8 \times 10^7$ S/m and thickness 0.035 mm. The final optimized geometry of the unit cell is given by: $a = 120$ mm, $t = 1$ mm, $r_1 = 46.8$ mm, $r_2 = 53.0$ mm, and $w = 2.2$ mm. The value of the capacitor added to the CLSRRs is $C = 270$ pF. For the sake of clarity, the simulation results of the retrieved effective permeability [31] of the proposed structure are given, as shown in Figure 3. It is obvious that our MM slab has a negative relative permeability $\mu = -1$ at the resonant frequencies around 16.30 MHz.
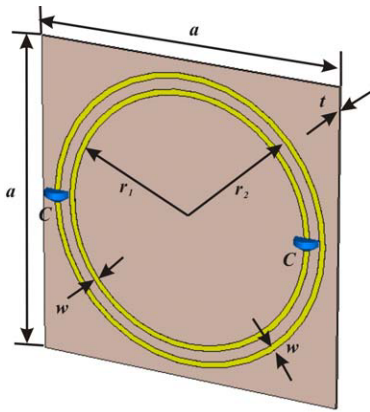

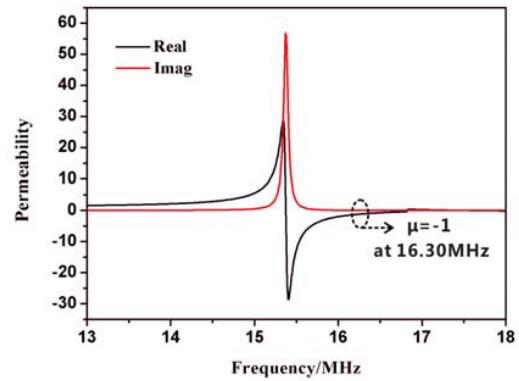**Figure 2.** Schematic diagram of unit cell of CLSRRs.

Figure 3. Simulated results of CLSRRs, retrieved effective permeability.

3. SIMULATION AND EXPERIMENTAL RESULTS

To verify the effect of the designed MM on the performance of WPT system, three cases, namely without MM, with one MM slab and with two MM slabs, are investigated. The WPT system model with two MM slabs is shown in Figure 4. Two slabs with 2×2 unit cells are put between the Tx and Rx coils. R is the inner radius of the helical copper coils, r_{in} the diameter of the copper wire, and l the distance between the two coils, respectively. d_1 and d_2 are variable. In this case, R is 10 cm, r_{in} 2.5 mm, and l 30 cm.
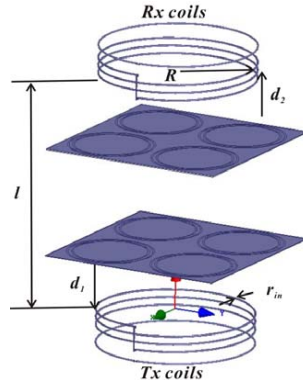
Figure 4. WPT system with MM slabs.
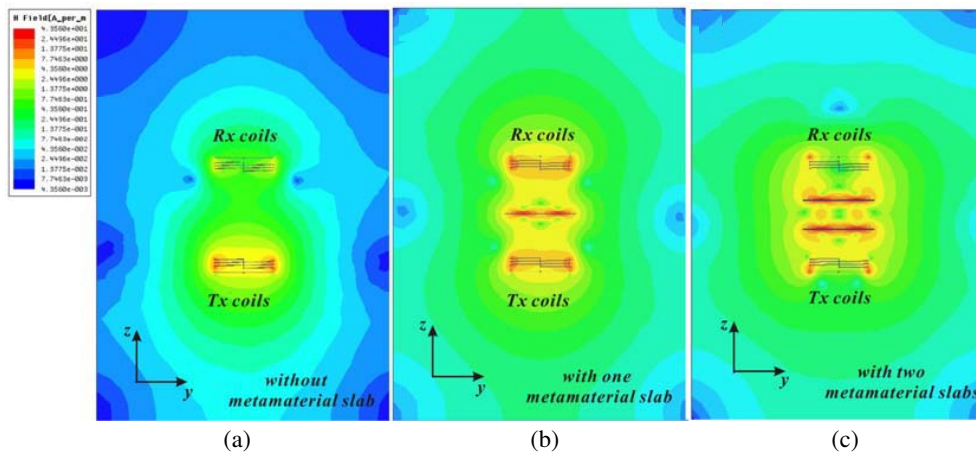

(a)　　　　　　　　　　　　　　　(b)　　　　　　　　　　　　　　　(c)

Figure 5. Comparison of magnetic field distribution of WPT system, (a) without MM slab, (b) with one MM slab, (c) with two MM slabs.

We observe the power transfer of systems with and without MM using the EM field simulator Ansoft HFSS. Figure 5 shows a comparison of the magnetic field magnitude distributions without MM, with one MM slab and with two MM slabs, respectively. Compared with the system without MM, the magnetic field intensity between the Tx and Rx coils with MM slabs is considerably increased, as shown in Figures 5(b) and 5(c). It is demonstrated that the magnetic field is enhanced and focused by the negative effective permeability MM slabs, which further verifies the validity of the theoretical analysis in Section 2. We also observe strong surface waves existing on both sides of the MM slab, which is responsible for the increased magnetic coupling [10].

Three cases of WPT system are simulated by the EM simulator for the linear magnitude scattering parameter $|S_{21}|$, which can be conveniently measured using a vector network analyzer (VNA). The effect of the position of the MM slab on the WPT is examined. The obtained results of the simulations are displayed in Figure 6. The values of $|S_{21}|$ are selected at the resonant frequencies in the simulations. It is obvious that the $|S_{21}|$ can be improved by using MM slab. Therefore, the whole simulated results indicate that a high-efficiency WPT system via magnetic resonance is implemented by using the CLSRRs structure as the magnetic flux guide. In the following section, the experiments are investigated using the proposed MM slabs, and more detail analysis will be given.

For experiments, as shown in Figure 7, we first fabricated the CLSRRs sample using the optimized dimensions by the conventional printed circuit boards (PCB) technology, and then loaded lumped capacitors to the structure by the welding technology. Finally, the fabricated slabs with different sizes were assembled, and the experimental sample was with 2×2 unit cells. Figure 8 depicts the setup of the metamaterial-based WPT system. An AV-3656A VNA (made by No. 41 Research Institute of China

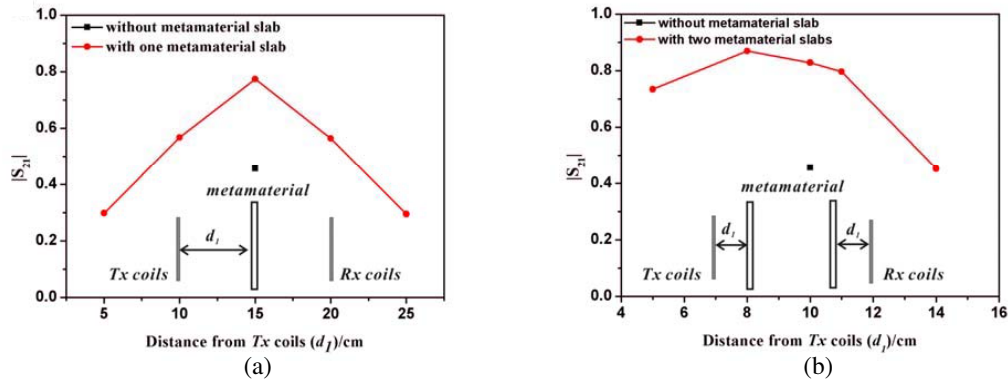**Figure 6.** $|S_{21}|$ versus the distance of the MM slab from Tx coils (d_1), (a) with one MM slab, (b) with two MM slabs.
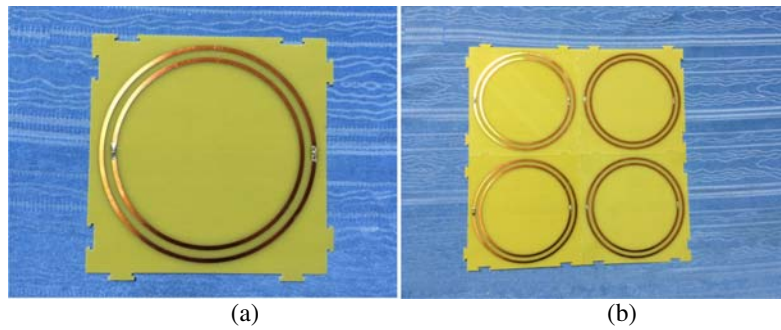

Figure 7. Photographs of the fabricated assembled CLSRRs slabs. (a) 1×1 unit cell, (b) 2×2 unit cells.
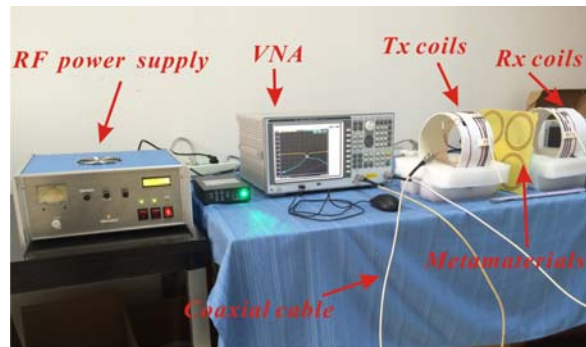

Figure 8. Photograph of the experiment setup of metamaterial-based WPT system.

Electronics Technology Goup Corp.) was used to measure the S-parameters of the WPT system. To verify the enhancement of the WPT system by using CLSRRs MM slabs, the four-coil systems integrated with one and two MM slabs are investigated by the experiments, respectively. The radio frequency (RF) power supply is a variable frequency power source with adjustable frequency range from 2 to 30 MHz. The maximum output power of the RF power supply is 100 W. The coaxial-like capacitors were used to adjust a target resonant frequency and to prevent variation of the target resonant frequency due to external objects.

It should be emphasized, in the following discussions, that the optimum efficiency will occur at different distances between the two MM slabs for different distances between the Rx and Tx coils.

First, according to the simulations, the two-coil resonators placed 30 cm apart were connected to VNA to evaluate PTE enhancement by MM slabs. For consistency, we characterize the relative power transmission of the WPT system using $|S_{21}|^2$ [16, 32]. The PTEs of WPT systems without MM, with one MM slab and with two MM slabs were measured, respectively. For simplicity, we only took the assembled 2×2 unit cells slab as an example in our study. Figure 9 shows the simulation and measurement results of transmission properties of the WPT systems with and without MM slabs. The PTE measurement results of the WPT systems meet well with the tendency of simulations. The frequency deviation between the experimental and simulated results may be due to the fabrication accuracy, measurement errors and the HFSS simulator accuracy in low MHz frequencies. According to the measured results, when one MM slab is used, the PTE improves 10% from 27.6% to 37.6%. When two MM slabs are used, we can adjust the gap spacing between the two slabs for the best performance. We note that the efficiency improves 17% from 27.6% to 44.6% with a 5 cm gap spacing.
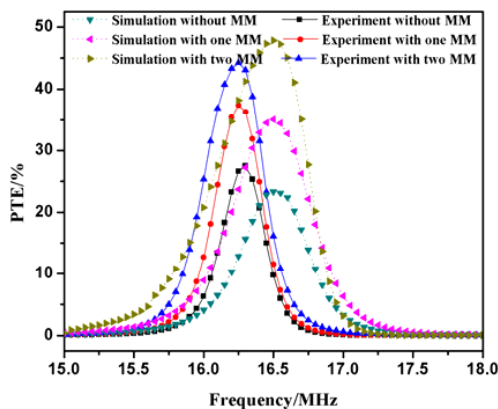

Figure 9. Comparison of simulation and measured PTEs in 3 different cases at a distance of 30 cm.
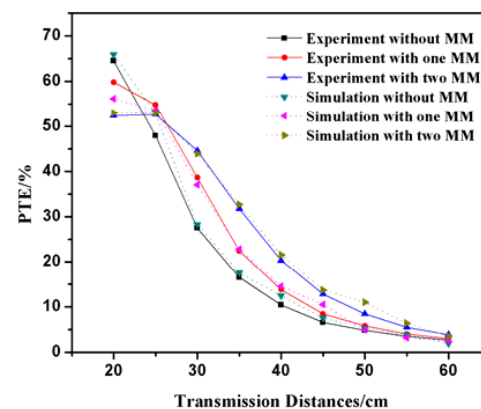
Figure 10. Comparison of simulation and measured PTEs versus transmission distances.

In order to examine the useful operating range of the WPT systems, the simulated and measured PTEs versus the transmission distance were also investigated in the cases of WPT systems both with and without MM slabs. As shown in Figure 10, the decrease rate of the PTE with the increasing of transmission distance of the WPT system with MM slabs is lower than that of the WPT system without MM. It is note that there are threshold distances above which the MM shows enhanced performance [9, 11, 20]. Compared with the case without MM, the CLSRRs structure starts to show better efficiency at the distance of 25 cm. So the thresholds distance for the MM slabs is about 25 cm, which is 2.5 times of the coil radius. The measured results confirm the theoretical calculation obtained using the coupled-mode theory [11]. Compared with the simulation results, we have obtained the consistent measurement results of the fabrication structures in the WPT systems. The deviation between the experimental and simulated results may be due to the actual radiation loss, fabrication accuracy, metamaterials' own loss, and measurement errors.

More practical WPT system with a light bulb load was investigated to directly verify the proposed transfer power enhancement. The rated voltage and power of light bulb are 24 V and 10 W. The light bulb was connected to the Rx coils as shown in Figure 11. The power was provided by the RF power supply as shown in Figure 8, and the input power was set to 25 W. The transmission distance maintained 30 cm, and the distances between the loop antennas and helical resonators were adjusted for optimal matching. The brightness of light bulb thus reflects the amount of power transferred. Three cases of the WPT system were demonstrated with and without MMs. The three corresponding pictures in Figure 11 were taken in the experiment at the same settings. Figure 11(a) shows the traditional system without MM, where the light bulb barely glows. It is obvious that the bulbs become much brighter in the system implemented MM slabs, as shown in Figures 11(b) and 11(c). All the experimental results reflect that PTEs of WPT system are indeed improved significantly by the MMs.
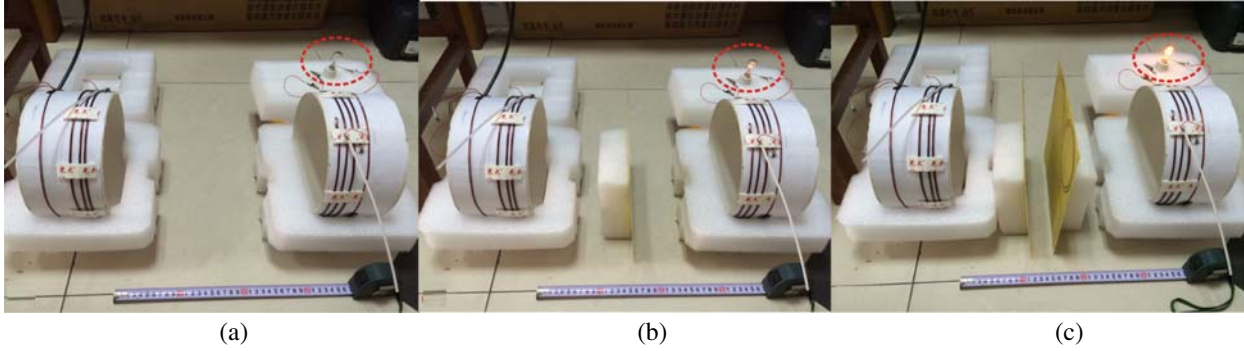
Figure 11. WPT experiment to a 10 W light bulb. Pictures are taken with same settings. (a) Traditional system without MM slab, (b) system with one MM slab, and (c) system with two MM slabs.

4. CONCLUSION

In this work, we have presented a simple, ultrathin, and assembled planar MM structure with lumped capacitors. The MM slabs of 2×2 unit cells with negative effective permeability at RF band are applied to WPT system for improvement of PTE. Simulated and experimental results show that the PTEs with one and two MM slabs have 10% and 17% improvement respectively at the transmission distance of 30 cm, compared with the case without MM slab. The measured PTEs of the systems at different transmission distances are also investigated. In addition, the proposed MM slabs are applied in a more practical WPT system (with a light bulb load) to reveal their effects. The results directly verify the efficiency improvement by the realized power received the load. The obtained result shows that the proposed MM slab, which has the advantages of light weight, ultrathin and fabrication simplicity, can find applications in the WPT technology.

ACKNOWLEDGMENT

REFERENCES

1. Tesla, N., *Electrical World and Engineer*, 21–24, January 7, 1905.
2. Garnica, J., R. A. Chinga, and J. Lin, "Wireless power transmission: From far field to near field," *Proc. IEEE*, Vol. 101, No. 6, 1321–1331, 2013.
3. McSpadden, J. O. and J. C. Mankins, "Space solar power programs and microwave wireless power transmission technology," *IEEE Micro. Mag.*, Vol. 3, No. 4, 46–57, 2002.
4. Kurs, A, A. Karalis, R. Moffatt, J. D. Joannopoulos, P. Fisher, and M. Soljacic, "Wireless power transfer via strongly coupled magnetic resonances," *Science*, Vol. 317, 83–86, 2007.
5. Sample, A. P., D. A. Meyer, and J. R. Smith, "Analysis, experimental results, and range adaptation of magnetically coupled resonators for wireless power transfer," *IEEE Trans. Ind. Electron.*, Vol. 58, No. 2, 544–554, 2011.
6. Pendry, J. B., "Negative refraction makes a perfect lens," *Phys. Rev. Lett.*, Vol. 85, 3966, 2000.
7. Zhang, X. and Z. Liu, "Superlenses to overcome the diffraction limit," *Nat. Mater.*, Vol. 7, No. 6, 435–441, 2008.
8. Merlin, R., "Radiationless electromagnetic interference: Evanescent-field lenses and perfect focusing," *Science*, Vol. 317, 5840, 927–929, 2007.

9. Urzhumov, Y. and D. R. Smith, "Metamaterial-enhanced coupling between magnetic dipoles for efficient wireless power transfer," *Phys. Rev. B*, Vol. 83, No. 20, 205114, 2011.

10. Huang, D., Y. Urzhumov, D. R. Smith, K. H. Teo, and J. Zhang, "Magnetic superlens-enhanced inductive coupling for wireless power transfer," *J. Appl. Phys.*, Vol. 111, No. 6, 064902, 2012.

11. Lipworth, G., J. Ensworth, K. Seetharam, D. Huang, J. S. Lee, P. Schmalenberg, T. Nomura, M. S. Reynolds, D. R. Smith, and Y. Urzhumov, "Magnetic metamaterial superlens for increased range wireless power transfer," *Sci. Rep.*, Vol. 4, 3642, 2014.

12. Zhao, Y. and E. Leelarasmee, "Controlling the resonances of indefinite materials for maximizing efficiency in wireless power transfer," *Microw. Opt. Techn. Lett.*, Vol. 56, No. 4, 867–875, 2014.

13. Huang, Y., H. J. Tang, E. C. Chen, and C. Yao, "Effect on wireless power transmission with different layout of left-handed materials," *AIP Adv.*, Vol. 3, No. 7, 072134, 2013.

14. Che, B. J., G. H. Yang, F. Y. Meng, K. Zhang, J. H. Fu, Q. Wu, and L. Sun, "Omnidirectional non-radiative wireless power transfer with rotating magnetic field and efficiency improvement by metamaterial," *Appl. Phys. A*, Vol. 116, No. 4, 1579–1586, 2014.

15. Choi, J. and C. H. Seo, "High-efficiency wireless energy transmission using magnetic resonance based on negative refractive index metamaterial," *Progress In Electromagnetics Research*, Vol. 106, 33–47, 2010.

16. Wang, B., K. H. Teo, T. Nishino, W. Yerazunis, J. Barnwell, and J. Zhang, "Experiments on wireless power transfer with metamaterials," *Appl. Phys. Lett.*, Vol. 98, No. 25, 254101, 2011.

17. Fan, Y., L. Li, S. Yu, C. Zhu, and C. H. Liang, "Experimental study of efficient wireless power transfer system integrating with highly sub-wavelength metamaterials," *Progress In Electromagnetics Research*, Vol. 141, 769–784, 2013.

18. Wang, B., W. Yerazunis, and K. H. Teo, "Wireless power transfer: Metamaterials and array of coupled resonators," *Proc. IEEE*, Vol. 101, No. 6, 1359-1368, 2013.

19. Rajagopalan, A., A. K. Ram Rakhyani, D. Schurig, and G. Lazzi, "Improving power transfer efficiency of a short-range telemetry system using compact metamaterials," *IEEE Trans. Microw. Theory Techn.*, Vol. 62, No. 4, 947–955, 2014.

20. Ranaweera, A. L. A. K., T. P. Doung, and J. W. Lee, "Experimental investigation of compact metamaterial for high efficiency midrange wireless power transfer applications," *J. Appl. Phys.*, Vol. 116, No.4, 043914, 2014.

21. Zhang, Y., H. Tang, C. Yao, Y. Li, and S. Xiao, "Experiments on adjustable magnetic metamaterials applied in megahertz wireless power transmission," *AIP Adv.*, Vol. 5, No. 1, 017142, 2015.

22. Wu, Q., Y. H. Li, N. Gao, F. Yang, Y. Q. Chen, K. Fang, Y. W. Zhang, and H. Chen, "Wireless power transfer based on magnetic metamaterials consisting of assembled ultra-subwavelength meta-atoms," *EPL-Europhys. Lett.*, Vol. 109, No. 6, 68005, 2015.

23. Rao, X. S. and C. K. Ong, "Amplification of evanescent waves in a lossy left-handed material slab," *Phys. Rev. B*, Vol. 68, No. 11, 113103, 2003.

24. Baena, J. D., L. Jelinek, R. Marqués, and F. Medina, "Near-perfect tunneling and amplification of evanescent electromagnetic waves in a waveguide filled by a metamaterial: Theory and experiments," *Phys. Rev. B*, Vol. 72, No. 7, 075116, 2005.

25. Cui, T. J., X. Q. Lin, Q. Cheng, H. F. Ma, and X. M. Yang, "Experiments on evanescent-wave amplification and transmission using metamaterial structures," *Phys. Rev. B*, Vol. 73, No. 24, 245119, 2006.
   2

26. Cho, Y., H. Kim, C. Song, J. Song, D. H. Kim, H. Kim, and J. Kim, "Ultra-thin printed circuit board metamaterial for high efficiency wireless power transfer," *IEEE Wireless Power Transfer Conference (WPTC)*, 2015.

27. Chabalko, M., B. Jordan, and R. David, "Magnetic field enhancement in wireless power using metamaterials magnetic resonant couplers," *IEEE Antennas Wireless Propag. Lett.*, Vol. 15, 2016.

28. Baena, J. D., R. Marques, F. Medina, and J. Martel, "Artificial magnetic metamaterial design by using spiral resonators," *Phys. Rev. B*, Vol. 69, No. 1, 014402, 2004.

29. Erentok, A., R. W. Ziolkowski, J. A. Nielsen, R. B. Greegor, C. G. Parazzoli, M. H. Tanielian, S. A. Cummer, B. I. Popa, T. Hand, D. C. Vier, and S. Schultz, "Lumped element-based, highly sub-wavelength, negative index metamaterials at UHF frequencies," *J. Appl. Phys.*, Vol. 104, No. 3, 034901, 2008.

30. Chen, W. C., C. M. Bingham, K. M. Mak, N. W. Caira, and W. J. Padilla, "Extremely subwavelength planar magnetic metamaterials," *Phys. Rev. B*, Vol. 85, No. 20, 201104, 2012.

31. Smith, D. R., D. C. Vier, Th. Koschny, and C. M. Soukoulis, "Electromagnetic parameter retrieval from inhomogeneous metamaterials," *Phys. Rev. E*, Vol. 71, No. 3, 036617, 2005.

32. Duong, T. P. and J. W. Lee, "Experimental results of high-efficiency resonant coupling wireless power transfer using a variable coupling method," *IEEE Microw. Wireless Compon. Lett.*, Vol. 21, No. 8, 442–444, 2011.